# Morphometric and sedimentological characteristics of Late Holocene earth hummocks in the Zackenberg Valley (NE Greenland)

Jesús Ruiz-Fernández[1], Marc Oliva[2], Xosé Luis Otero[3], Cristina García-Hernández[1]

[1] Department of Geography, University of Oviedo, Spain

[2] Department of Geography, Universitat de Barcelona, Catalonia, Spain

[3] CRETUS institute. Departamento de Edafoloxía e Química Agrícola, Facultade de Bioloxía, Universidade de Santiago de Compostela, Spain.

**Corresponding author**

Jesús Ruiz-Fernández, Department of Geography, University of Oviedo. C/ Amparo Pedregal s/n, 33011, Oviedo, Asturias, Spain.

Email: ruizjesus@uniovi.es

**Abstract**

A multi-approach characterization of three earth hummock fields has been conducted to understand the morphometrical characteristics and distribution pattern of these periglacial features in the Zackenberg Valley, NE Greenland. Earth hummocks develop in poorly-drained areas affected by intense cryogenic conditions. An accurate analysis of the morphometrical properties of hundreds of earth hummocks distributed between different Early Holocene moraine systems of the eastern slope of the Zackenberg Valley reveals an important control of microtopography on their distribution. Sedimentological analysis of selected earth hummocks shows evidence of alternating organic-rich layers and mineral units. Radiocarbon dates of the basal organic layers in contact with the permafrost table yielded ages 615 ± 25 and 1755 ± 60 cal yr BP, with lower sedimentation rates over the last centuries when soil formation prevailed. Geochemical analysis of the soils (Glacic Reductaquic Cryosols) showed also significant differences in the properties and composition among the soils of the different fields of hummocks.

**Key words**: NE Greenland, Zackenberg Valley, earth hummocks, Late Holocene, morphometry, Cryosol.

## 1. Introduction

Several periglacial landforms such as rock glaciers (e.g. Aoyama, 2005; Winkler and Lambiel, 2018), ice-wedge polygons (Burn, 1990; Oliva et al., 2014), or solifluction lobes (e.g. Elliott and Worsley, 1999; Oliva et al., 2011) have been successfully used to reconstruct past environmental conditions. Other periglacial landforms such as earth hummocks can also provide valuable information for this purpose. This term was first used by Sharp (1942) to define dome-shaped periglacial features typical of poorly-drained environments (French, 2007). Several mechanisms are involved in their formation, including cryoturbation, cryostatic and hydrostatic pressure, differential frost heave and the cellular circulation model (Grab, 2005a, 2005b). As a result, the internal structure of earth hummocks reveals a polygenic development, with alternating mineral sediments and peat or organic-rich layers affected by frost activity (Van Vliet-Lanoë and Seppälä, 2002). Indeed, the internal structure is the result of translocation of surface horizons. Earth hummocks are highly dependent on variations in thermal regime, snow thickness and precipitation (Luoto and Seppälä, 2003), and their internal sedimentary sequences can also be used to trace past environmental and climatic conditions (Ellis, 1983). The development of these miniature frost-induced mounds is also related to the vegetation cover.



Research on earth hummocks has generated interest within the scientific community studying permafrost and periglacial processes. Several studies have been carried out since the mid-1970s focusing mainly on their sedimentary structure (Tarnocai and Zoltai 1978; Pemberton, 1980; Scotter and Zoltai, 1982; Grab, 2005b; Kokelj et al., 2007; Pintaldi et al., 2016), geochronology of their formation (Ellis, 1983; Van Vliet-Lanoë and Seppälä, 2002), ground thermal regime (Costin and Wimbush, 1973, Tarnocai and Zoltai 1978;

Grab, 2005a, 2005b; Scott et al., 2008), hypotheses about their formation, evolution and disintegration (Mackay and MacKay, 1976; Tarnocai and Zoltai 1978; Mackay, 1980; Grab, 2005a, 2005b; Seppälä, 2005; Killingbeck and Ballantyne, 2012; Gurney and Hayward, 2014), their implications on hillslope drainage (Quinton and Marsh, 1998; Ogata, 2007), and their relationships with vegetation and/or topography (Zoltai and Pettapiece, 1974; Kojima, 1994; Luoto and Seppälä, 2002, 2003; Ogata, 2005; Pintaldi et al., 2016). The morphometry of earth hummocks has been also subject of research (Pemberton, 1980; Kokelj et al., 2007; Killingbeck and Ballantyne, 2012). More recently researchers focused on the relationship between these features and soil organic carbon content, as well as with the potential release of greenhouse gases stored in the active layer (Gillespie et al., 2014; Verret et al., 2019). However, the use of earth hummocks as a paleoenvironmental archive to reconstruct past environmental and climatic conditions has been scarcely used (e.g. Tarnocai and Zoltai, 1978; Scotter and Zoltai, 1982; Ellis, 1983; Verret et al., 2019).

Earth hummocks are distributed in a wide variety of environmental settings, including polar and mountain regions (Grab, 2005b). Main studies have focused on several Arctic and sub-Arctic areas, such as Canada (e.g. Kojima, 1994; Quinton and Marsh, 1998; Kokelj et al., 2007), Lapland (e.g. Van Vliet-Lanoë and Seppälä, 2002; Seppälä, 2005), Iceland (e.g. Gerrard, 1992), and Norway (e.g. Gurney and Hayward, 2014). Earth hummocks have been also examined in a wide range of mountain environments such as the Snowy Mountains in Australia (Costin and Wimbush, 1973), Italian Alps (Pintaldi et al., 2016), the Cumbria and Dartmoor plateau in England (Pemberton, 1980; Kilingbeck and Ballantyne, 2012), regions of Vlasina and Krajište in Southern Serbia (Milošević et al., 2007), the Nemuro Peninsula and Nikko National Park in Japan (Ogata, 2005, 2007), Old Man Range in New Zeland (Scott et al., 2008), and the Mashai Valley in Lesotho (Grab, 2005a).

Our current understanding of earth hummocks still presents some uncertainties with regards to the genesis and development cycle of these features (Grab, 2005b). Therefore, further research is needed to characterize these abundant features in the landscape of the rapidly changing cold-climate regions, namely in the Arctic. Thus, the aim of this research is to characterize the Late Holocene environmental evolution in the lowlands of the Zackenberg Valley based on the geomorphological, sedimentological, geochronological and geochemical analysis of earth hummocks. This will be done by answering the following specific objectives: i) examining the morphometric properties of several fields of earth hummocks distributed at different elevations constrained by moraine system (MS), including the discussion of the variables that control their dimensions and morphology and ii) presenting a detailed sedimentological characterization of several of these periglacial features in order to evaluate their internal lithostratigraphical composition.



## 2. Study area

The study sites are located in the vicinity of the Zackenberg Polar Research Station (74º28'11.50''N, 20º34'24.58''W), namely on the eastern slopes of the Zackenberg Valley connecting with Aucella Peak (985 m a.s.l.; Figure 1). This area is included within the National Park of Northeast Greenland. The bedrock across the Zackenberg Valley and its surroundings is composed of heterogeneous materials, mainly of Precambrian orthogneiss, Jurassic and Cretaceous sedimentary rocks (mudstones, sandstones and conglomerates), as well as Tertiary basaltic lavas (Higgins, 2003; Pedersen et al., 2013).

Figure 1

During the Last Glacial Maximum (LGM) the entire area was covered by the Greenland Ice Sheet (Vasskog et al., 2015; Sinclair et al., 2016), with valleys filled with hundreds of meters of ice. Ice streams flowing along deep U-shaped glacial valleys grounded tens of kilometers offshore the present-day coastline. The deglaciation of the valley floor started during the onset of the Holocene prior to 11 ka cal BP (Wagner, et al., 2010; Bennike and Wagner, 2012) and the Zackenberg Valley, where our study sites are distributed, was deglaciated during a warmer period around ca. 8 ka (Vinther et al., 2009; Cable et al., 2018). The regional present-day landscape of the study area includes deep fiords, U-shaped valleys, steep ravines and glaciated plateaus at 1000-1600 m a.s.l. forming small ice caps (e.g. Payer Land, A. P. Olsen Land and Clavering Ø). Currently, intense periglacial dynamics prevail in ice-free environments and conditions terrestrial ecosystem dynamics. Permafrost is continuous across the ice-free areas with a thickness up to 400 m (Brown et al., 1997; Christiansen et al., 2008; Westermann et al., 2015). On the other hand, maximum active layer thickness at the end of the thaw season varies between 40 cm and more than 200 cm, with an increase of 0.8 to 1.5 cm/yr from 1996 to 2012 (Elberling et al., 2013).



Climatically, the Zackenberg Valley is situated within the High Arctic Zone (Kottek et al., 2006), within a transition zone between the Greenland Ice Sheet (W) and the North Atlantic Ocean (E). The mean annual air temperature (MAAT) from 1996 to 2015 was -9.0 ºC, with a yearly average precipitation of 367 mm and large inter-annual variation (Højlund Pedersen, 2017). Up to 90% of the annual precipitation falls in the form of snow

(Hansen et al., 2008). Positive monthly average temperatures are only recorded in June, July and August (Sigsgaard et al., 2009). The average maximum snow depth was 0.81 m (1997-2009), although it varied significantly, with a maximum of 1.33 m (2001-2002), and a minimum of 0.17 m (2008-2009; Sigsgaard et al., 2009).

Vegetation is scarce, with tundra mostly limited to the areas of flat topography and greater soil development in the valley floors. It consists of grasslands, fens and interspersed snow patches. It is dominated by plants such as *Cassiope tetragona* and *Salix arctica* (Bay, 1998). Tundra gradually becomes more open in slopes and at higher elevations. As a result of the presence of permafrost, poorly drained areas are abundant in the Zackenberg Valley floor. During the vegetation growing season, water supply is controlled by the existence of large snow patches that melt gradually as temperatures rise (Westermann et al., 2015).

The glacier outlet that occupied the Zackenberg Valley during the LGM was a tributary of the Tyroler Fjord. The valley deglaciation generated at least five MS distributed at different altitudes on the slopes of the eastern part of the Zackenberg Valley. Subsequently, due to the abundance of melting water with underlying permafrost, several fields of earth hummocks developed on these slopes.



## 3. Methodology

Three earth hummocks fields (EHFs) located on the eastern slope of the Zackenberg Valley have been studied from the morphometric, sedimentological, geochronological and geochemical point of view. Fieldwork was carried out in the beginning of August 2018 during the early thaw season after a cold and snowy year in NE Greenland. Field activities consisted in the morphometrical characterization of earth hummocks and the geomorphological setting of each of these fields, as well as in the collection of samples and data for morphometry, geochronology, sedimentology and geochemical analyses.

### 3.1. Morphometry

We examined the morphometrical characteristics of 40 earth hummocks in each of the study sites along a vertical sequence (EHF-1, EHF-2, EHF-3), for a total of 120 landforms. The sample size exceeds the minimum number of observations that, by consensus within the statistical community (Sullivan and Woodall, 1996), is considered necessary to obtain reliable results. Morphometrical characteristics were determined based on several quantifiable parameters, such as length (L), width (W), maximum height (H1), as well as the depth of the active layer at the top of the earth hummocks (AL-TOP) and in the inter-hummock area (AL-BASE). Derived morphometric parameters such as L/W, L/H1, W/H1, AL-TOP/H1 and AL-BASE/H1 ratios have been calculated. The qualitative parameters were based on field observations considering two different aspects of the earth hummocks: Their geometric shape (circular, elliptical, crescent or irregular), and the direction of the major axis of each hummock (longitudinal, diagonal or perpendicular) with respect to the direction of the drainage of the slope.



### 3.2. Sedimentology and geochronology

In each field, one representative earth hummock was opened to characterize its sedimentological composition. We collected six organic-rich samples (bulk sediment) to conduct $^{14}C$ AMS (Accelerated Mass Spectrometry) dating at the Radiochronology Laboratory of the *Centre d'Études Nordiques* (Laval University, Canada; Table 1).

Results were converted in calibrated years using the CALIB program (Stuiver and Reimer, 1993), version 7.0.2 based on the data set IntCal13 (Reimer et al., 2013).

### 3.3. Soil analysis

Samples were stored in plastic bags and transported to the laboratory at approximately 4 °C. Once in the laboratory, one portion of each soil sample was dried at 45 ºC and sieved through a 2 mm mesh. The remaining subsamples were kept frozen at -18 ºC and used for fractioning of Fe, Mn and trace metals (Co, Cu).

Duplicate determinations were made of pH in water (pHw at a ratio of 1:2.5,10 g soil: 25 ml distilled water) and electric conductivity (EC at a ratio of 1:5, 10 g soil: 50 ml distilled water); (Rowell, 1994) and of particle size distribution (by the pipette method: Gee and Bauder, 1986). The total organic carbon (TOC), after removal of carbonates with 10% HCl (Cannone et al., 2008), and total nitrogen (TN) were measured in a ThusPec autoanalyzer. The total concentration of metals was also extracted in duplicate by adding 8 ml of a mixture of $HNO_3$/HCl (3:5, v/v) in a 120 ml Teflon bomb containing 0.5 g of previously dried and ground soil (Otero et al., 2016) and heating the mixture in an Ethos Plus microwave lab station. The efficiency of the extraction process (>92%) was determined by analysis of certified reference material (MESS-3 and Soil SO3).

Three metal fractions were also extracted: 1) metal pyrophosphate (MePy; Me=Fe, Mn) extracted with sodium pyrophosphate (0.1M; soil:extractant ratio 1:100, 16 hours shaking); (Bascomb, 1968), 2) metal oxalate (MeOx) extracted with acid ammonium oxalate (0.2M, pH 3); (soil:extractant ratio 1:100, 4 hours shaking); (Blakemore, 1983), and 3) metal dithionite (MeD) extracted with citrate bicarbonate dithionite of sodium (soil:extractant 1:20; 30 min shaking); (Mehra and Jackson, 1960). Metal pyrophosphate provides an estimate of the metal-organic complexes (Bascomb, 1968; Violante et al., 2010); the difference between metal oxalate and metal pyrophosphate provides an estimate of amorphous iron oxyhydroxides (Blakemore, 1983), while the difference between metal dithionite and metal oxalate provides an estimate of crystalline iron oxyhydroxides (Mehra and Jackson, 1960).

Macro (P) and micronutrients (Fe, Mn Co, Cu) were extracted by the Mehlich-III method (Mehlich, 1984). The Mehlich-III extraction solution consisted of 2M $CH_3COOH$, 0.25M $NH_4NO_3$, 0.015M $NH_4F$, 0.013M $HNO_3$ and 0.001M EDTA. The concentrations of Fe, Al, Mn, Cu, and Co in each extract were determined by atomic absorption spectrometry (Perkin-Elmer model), while Mehlich P was determined by the blue molybdenum method (Murphy and Riley, 1962).

Dissolved organic carbon (Cw) was extracted from the fresh soil samples with Milli-Q water (soil:solution ratio, 10 g soil:100 ml water); (Otero et al., 2013). The samples were maintained at room temperature, with continuous shaking for 1 h. The extracted was analysed in a loop flow analysis system (Systea).

### 3.4 Statistical analysis

A descriptive statistical analysis of earth hummocks from a morphometric point of view was carried out with absolute and relative frequency tables, distribution analysis using box-plots, and statistical inference using linear regression models and correlation between the variables. All statistical analyses were performed using R version 3.6.3. On the other hand, soil data were jointly analysed for each section and compared among sections. Differences among sections were established by one-way ANOVA followed by a Holm-

Sidak test. Correlation between TOC and TN was examined using Spearman's coefficient. Correlation was considered significant at the 5% probability level. Tests were performed using the Sigma Plot 11.0 software.

## 4. Results

### 4.1. Geomorphological context of EHFs and field observations

The EHF-1 (74º 27' 16.5" N, 20º 29 '17.5" W; 127 m a.s.l) constitutes the highest field in the eastern slope of the Zackenberg Valley including well-developed earth hummocks. This field shows a gentle slope of 5º between the MS-5 and MS-4 (Figure 2). The MS-5, located upslope the EHF-1, is eroded by several streams. Some moraine boulders are being remobilized by solifluction processes, forming even ploughing boulders. In fact, some large glacial erratic boulders are found in the middle of EHFs. A large snow field was still present at the foot of MS-5 in summer 2018, where the EHF-1 is located. Consequently, the soil surface of the area was saturated by water and flooded, even with superficial drainage in some sectors. Vegetation consists of grasses, with the presence of mosses and *Salix arctica*.

Figure 2

The EHF-2 (74º 28' 56.9" N, 20º 29 '59.4" W; 61 m a.s.l) is located between MS-4 and MS-3 distributed on a slope of 4º. Soil surface was much less saturated than in EHF-1. Coalescent earth hummocks are more abundant in this field than in the others. Irregular–shaped features are widespread, mostly due to the coalescence of several earth hummocks. Vegetation cover is mainly composed of grasses, but there are also moss mats on the top of some earth hummocks. These hummocks had a thinner active layer than those covered by grass formations. In some well-developed earth hummocks, cracks are visible on the surface revealing an initial stage of partial collapse of these periglacial landforms.

The EHF-3 (74º 27' 49.1" N, 20º 30 '15.9" W; 42 m a.s.l) is located between the MS-3 and MS-2, in a relatively flat area of 3º slope. The earth hummocks in this field are smaller than in the EHF-2. As a result of the presence of abundant late-lying snow patches and lower slope inclination, soil saturation was higher in this field than in the EHF-2 and the inter-hummocks area was frequently flooded. Here, vegetation was mainly composed of grasses and *Salix arctica*.

### 4.2. Morphometry of earth hummocks

The average length and width of the hummocks are 77 cm (Figure 3B) and 58 cm (Figure 3C), respectively. The average maximum height is 22 cm (Figure 3D). The EHF-2 includes the landforms with greater length and width, as well as maximum height. Likewise, in the EHF-1 all measurements of position for the variables length and width (i.e. average, percentiles and quartiles) indicate the shortest length and width of the EHF-1 landforms. There are no noticeable differences in the maximum height of the features between the EHF-1 and the EHF-3. The examined hummocks show mainly elliptical forms. Specifically, there is a linear relationship between length and width that can be expressed as follows: L=1.31*W (Figure 4A).

Figure 3

Figure 4

The L/W ratio does not show remarkable differences between the EHF-1, EHF-2 and EHF-3, being favourable for the length in all of them, although it is less clear in the TF-3, in which the shapes would be less lengthened (Figure 3A). The earth hummocks that were classified in the field as irregular (coalescent features) stand out as those showing the highest values of maximum height (Figure 5), and there is a positive linear relationship between the ratio L/W and H1 in elliptical features (Figure 4B). Moreover, the hummocks in which the longitudinal axis showed a longitudinal direction with respect to the drainage flow show the maximum heights, while those in which the axis showed a perpendicular direction were the most lengthened (Figures 6A and 6B).

Figure 5

Figure 6

In half of the examined earth hummocks the direction of the axis was perpendicular to the drainage flow, followed by the diagonal and longitudinal direction (53%, 25% and 22%, respectively). This trend is observed in the three EHFs, although it is clearer in the EHF-3 (62%, 23% and 15%, respectively).

The average thickness of the AL-TOP is 39 cm. No substantial differences were detected between the three EHFs, with a larger variability in the EHF-2 (Figure 3E). The AL-BASE is 27 cm, and the EHF-2 shows the highest AL-BASE values (Figure 3F). Finally, there is no relationship between AL-TOP and H1 (Figure 4C), nor between AL-BASE and H1 (Figure 4D).

### 4.3. Sedimentology and geochronology of earth hummocks

Three profiles of earth hummocks from each of the fields were examined to explore past environmental changes in the area (Figure 7):

Figure 7

**EH-1**

We excavated a 0.5 m deep section of an earth hummock in the EHF-1 (74º28'56.9''N–20º 29'59.3''W, 72 m a.s.l.) down to the permafrost table. This landform included four different lithostratigraphical units:

EH-1.1 (0-4 cm). Bottom layer highly organic-rich layer (TOC: 4.9%). The base of the layer was radiocarbon dated, reporting an age of 1755 ± 60 cal yr BP (Table 1).

EH-1.2 (4-25 cm). Mineral sandy unit with a sharp decrease of organic matter content (TOC: 2.1%).

EH-1.3 (25-30 cm). Sandy (sand: 59%) layer with gradual increase of organic matter with the presence of small roots (TOC: 6.7%).

EH-1.4 (30-50 cm). Increasing organic matter to the current topsoil (TOC: 4.3-5.4%). The base of the layer at 30 cm depth yielded an age of 1300 ± 25 cal yr BP.

**EH-2**

A 0.38 m deep section was excavated in an earth hummock from the EHF-2 (74º28'56.8''N–20º29'59.4''W, 62 m a.s.l.) until the frozen layer. This feature includes five different lithostratigraphical units:

EH-2.1 (0-4 cm). Bottom layer slightly brownish sandy (sand: 71%) unit with low content of organic matter (TOC: 0.32%). The base of this unit yielded an age of 940 ± 20 cal yr BP (Table 1).

EH-2.2 (4-8 cm). Sandy (sand: 62%) layer with reddish mottles (2.5YR 4/8, Soil Munsell colour chart) and considerable organic matter content (TOC: 22%).

EH-2.3 (8-17 cm). Silty (silt: 46%), greyish layer (2.5Y 4/6) with high content of organic matter (TOC=5.8%).

EH-2.4 (17-24 cm). Sandy (sand: 51%) and organic rich layer (TOC: 5.5%) with some gravels (Ø < 2 cm). The base of this unit at 18 cm depth reported an age of 495 ± 20 cal yr BP.

EH-2.5 y EH-(24-38 cm). Dark brown (2.5Y 4/1) unit, with increasing organic matter (TOC: 11.6%) and abundant roots.

**EH-3**

We excavated a 0.29 m deep section in an earth hummock from the EHF-3 (74º28’48.1’’N-20º30’15.0’’W, altitude 53 m a.s.l.). The profile shows three different lithostratigraphical units down to the frozen level:

EH-3.1 (0-8 cm). Silty mineral unit (silt: 55%), with high organic matter content (TOC: 10.3%) and the presence of oxyhidroxides of iron mottels (2.5YR 4/8) at the top. The base has been dated at 615 ± 25 cal yr BP (Table 1).

EH-3.2 (8-11 cm). Highly rich organic layer (TOC: 25%) that has been dated as modern at 9 cm depth.

EH-3.3 (11-29 cm). Very organic-rich layer (TOC: 33.7%) with abundant decomposed roots.

### 4.4. Soil characterization

#### 4.4.1. Soil properties and composition

The profile of the three EHs showed clear morphological evidence of gleyic properties in mineral horizons. The presence of grey mottles (5Y 4/1 when moist) on an olive brown (2.5Y 4/6), olive yellow (2.5Y 6/6), or greenish grey soil matrix (10GY 6/1), suggesting reducing conditions.

On the other hand, red (2.5YR 4/8) or yellowish red (5YR 5/8) mottles corresponding to areas of the profile with oxymorphic zones where Fe precipitates as Fe oxyhydroxides (IUSS Working Group WRB, 2006).

Mean pH values were slightly acidic (mean values: pH: 5.7-6.3; Table 2), but it should be noted that the uppermost horizons of profiles EH-1 and EH-2 were clearly more acidic (pH: 5.1-5.4) than the deeper horizons (pH: 6-6.9). Furthermore, profiles EH-1 and EH-2 were significantly more acidic than EH-3. (Table 2; Supplementary material).

Electric conductivity showed very low mean values (EC<215 µS $cm^{-1}$) in the three profiles. However, ion concentration in field EH-3 was significantly higher than in the other two.

Granulometric composition also varied in different EHFs. The EH-1 and the EH-2 showed a coarser texture (loamy sand; Table 2; Supplementary material) dominated by the sand fraction (53-54%), while EH-3 showed a loamy silt texture, with silt as the dominant fraction (54±5.6%). It is worth highlighting that granulometric composition showed major changes with depth. Thus, the highest percentages of sand fraction were obtained in samples from the top and bottom of each profile, while the clay fraction showed an inverse pattern (Supplementary material).

Table 2

Likewise, TOC content greatly oscillated with depth. TOC was extremely high in EH-3 at all depth levels, but particularly in the surface ($TOC_{sup}$: 33.7%; Supplementary material), corresponding to an Histic horizon formed by partially decomposed organic remains. Sections EH-1 and EH-2 showed significantly lower values (mean TOC values: 4.7-5%). Organic carbon soluble in sodium pyrophosphate (CPy) was similar for the three sites (Table 2); conversely, water-soluble organic carbon (Cw) was significantly higher in profile EH-3 (Cw: 1072±358 mg $kg^{-1}$) than in the other two (Cw: 72-110 mg $kg^{-1}$). Total nitrogen followed a similar pattern to TOC, with significantly higher values in profile EH-3 (TN: 1.1±0.3%) than in the other profiles (TN~ 0.3%). The high correlation between TOC and TN (rs: = 0.965, $p<0.001$, n=14) suggests that most of the TN corresponds to organic N.



**4.4.2. Total Al, Fe, and Mn concentrations**

Mean total concentration of Al and Fe was similar in the three profiles (Table 3), which indicates that the geological substrate is similar. However, total Mn (TMn) concentration showed extremely high values in EH-3 (TMn: 8227±8092 mg $kg^{-1}$) compared with profiles EH-1 and EH-2 (TMn: 463-709 mg $kg^{-1}$), which in this case indicates a mobilization of Mn from the highest to the lowest areas of the landscape.

**4.4.3. Partitioning of Fe and Mn**

Mean concentration of Fe associated with organic matter in soil (FePy) was similar among the three sites, but Mn showed significantly higher values in section EH-3 (MnPy: 4029±4220 mg $kg^{-1}$; Table 3), particularly in the two upper levels (Supplementary material). Mean content of amorphous Fe oxyhydroxides (FeOx) and crystalline oxyhydroxides Fe (FeD) was similar in the three sections, with mean concentration ranges of 0.21-0.33% and 0.57-0.79%, respectively. However, it is worth noting the high concentrations of FeOx compared with FeD, which is in accordance with oxymorphic conditions observed.

#### 4.4.4. Bioavailable of macro- and micronutrients and micronutrients associated to organic matter

Total phosphorus content was low (TP<100 mg $kg^{-1}$) in all samples and was similar among sites; however, bioavailable P (PMe) showed significant differences. Concentration of PMe was extremely low in EH-1 and EH-2 (PMe: 0.62-1.10 mg $kg^{-1}$), while in EH-3 it was 10 to 18 times higher (PMe: 11±8 mg $kg^{-1}$); (Table 4). Similarly, FeMe and MnMe were also very high in EH-3 in relation to EH-1 and EH-2 profiles, but only MnMe was significantly higher (Table 4).

Content of TCo was significantly higher in EH-3 (61±42 mg $kg^{-1}$) than EH-1 and EH-2 (mean values: 18-21 mg $kg^{-1}$), whereas TCu (mean values TCu: 49-55.4 mg $kg^{-1}$) did not show significant differences among sites, although the results showed a high enrichment of copper in the subsurface layer in EH-3 (Table 4). The bioavailability fraction of Co (CoMe) was significantly higher in EH-3 (CoMe: 3.38±2.8 mg $kg^{-1}$); than EH-1 and EH-2 profiles (CoMe: 0.7-0.9 mg $kg^{-1}$); whereas CuMe did not show significant differences among sites but with higher values in EH-3 (CuMe: 10±14 mg $kg^{-1}$) than EH-1 and EH-2 (mean values CuMe: 2.8-7.0 mg $kg^{-1}$) (Table 4).

Finally, the metal fraction concentration associated to organic matter (metals soluble pyrophosphate) did not show differences among profiles (CoPy: EH-1: 2.3±0.8; EH-2: 1±0; EH-3: 19±11 mg $kg^{-1}$; CuPy: EH-1: 14±6; EH2: 8.4±4.9; EH-3: 18±9 mg $kg^{-1}$), but again the concentrations of EH-3 were higher (Table 4).

## 5. Discussion

Geomorphological, morphometrical and soil data of earth hummocks reveal some remarkable differences that can provide insights into their recent forming processes as well as into the past climatic and environmental evolution in the Zackenberg Valley.

### 5.1. Late Holocene development of earth hummocks

In NE Greenland, the large Quaternary glaciers grounded onto the outer continental shelf started to retreat during the LGM at ca. 22 ka cal BP (Ó Cofaigh et al., 2004; Winkelmann et al., 2010). Following the glacial expansion during the Younger Dryas cold period, warmer conditions favoured ice retreat and glaciers remained confined within the fjords (Bennike et al., 2008). The Zackenberg Valley floor has been ice-free during most of the Holocene as the oldest post-glacial sediments were dated at 10.1 ka cal BP (Christiansen et al., 2002). Glacial retreat favoured the formation of a large delta at the outlet of the Zackenberg River (Gilbert et al., 2017) and left a sequence of moraine ridges in the slopes of the valley. Post-glacial slope processes have reworked these moraines leaving smoothed remnants of these ridges. In between the lowest moraine ridges, there are the earth hummock fields that have been examined in this paper (Figure 2). The radiocarbon dates of the lowest sediments observed in three earth hummocks (EH-1 to EH-3) have revealed ages ranging between 615 ± 25 and 1755 ± 60 cal yr BP (Figure 7). Therefore, these landforms are relatively young features in this ice-free periglacial landscape, which must have undergone large environmental changes following the large Holocene climate oscillations occurred in the High Arctic region (Briner et al., 2016). In addition, the difference of the basal radiocarbon dates between the earth hummocks in neighbouring sites must be also framed within the pattern of development and dynamics of these features (Kokelj, et al., 2007).

The intense cryoturbation processes in this permafrost environment (Christiansen et al., 2008) accelerate the collapse and re-development of these periglacial landforms, and therefore, important age differences can be found in earth hummocks distributed in close sites. In addition, radiocarbon dates in earth hummocks can be affected by the vertical translocation of fine-grained particles (including datable organic matter fragments) induced by cryoturbation processes. Thus, care needs to be taken when interpreting radiocarbon dates from these features.

Climate variability increased in the Northern Hemisphere during the second half of the Holocene (Mayewski et al., 2004; Wanner et al., 2014), including in the Arctic, where a long-term cooling trend is detected since the Neoglacial period (Briner et al., 2016). The onset of this climate pattern shows a time-transgressive pattern across the region (McKay et al., 2018). The first dated earth hummocks in the Arctic region correspond to this period. Earth hummocks of Mid Holocene age started forming in areas of North America between 5 and 2.5 ka cal BP (Tarnocai and Zoltai, 1978) as well as in Norway between 4.8 and 3 ka cal BP (Ellis, 1983). The basal ages of the earth hummocks in the Zackenberg

Valley are therefore of Late Holocene age, being younger than 2 ka cal BP, which is very similar to the pattern reported in Lapland and northern British Columbia (Van Vliet-Lanoë and Seppälä, 2002; Verret et al. 2019).

The internal structure of the earth hummocks reveals an alternation of mineral layers and organic-rich units. These variations must have been driven by Late Holocene climate variability: whereas the deposition of mineral sandy-silty sediments reveal slopes affected by active mass-wasting processes, peat formation suggests prevailing geomorphic stability. In cold-climate environments such as in the Zackenberg Valley, colder and/or wetter phases favour the mobilization of soil particles in poorly vegetated slopes, whereas warmer temperatures favour a longer summer season enhancing soil formation (Oliva et al., 2011; Oliva and Gómez-Ortiz, 2012). The formation of the organic-rich layer covering the top of these landforms in the Zackenberg Valley took place during the last millennium, as also occurred in Lapland (Van Vliet-Lanoë and Seppälä, 2002). Climate conditions can trigger complex feedbacks in a tundra environment such as the Zackenberg Valley that can affect soil frost and vegetation cover, which in turn, can affect the formation of collapse earth hummocks as well as the rates of peat formation covering these features. Earth hummocks in the Zackenberg Valley recorded higher rates during phases with mineral deposition (0.43-0.64 mm $yr^{-1}$) than during phases with organic-rich soil formation (0.15-0.36 mm $yr^{-1}$). However, the small number of radiocarbon dates impedes inferring any climate control on these sedimentation rates.



**5.2. Topographical and geomorphological controls on the distribution and morphometrical parameters of earth hummocks**

Together with the moisture availability and the presence of frost-susceptible soils (Grab, 2005a; Gurney and Hayward, 2014), the topographical and geomorphological context has a clear influence on the development of earth hummocks controlling water drainage, soil formation, active layer thickness, etc. Surface drainage occurs through the interhummock sectors, as well as subsurficially along the unfrozen saturated layers in these microtopographically depressed areas (Quinton and Marsh, 1998). This subsurface circulation results in channels oriented downslope with a low hydraulic conductivity due to the attenuating action of the flow exerted by the hummocks (Quinton and Marsh, 1998). In addition, several studies have shown the important influence of the microtopography of earth hummocks on soil properties, pedogenesis and vegetation distribution, and significant differences on the same parameters have been found between hummocks and interhummocks (Pintaldi et al., 2016).

The EHF-1 includes the smallest hummocks in terms of length, width and height. Its location at a higher altitude at the foot of the MS-5 and steeper inclination than the other EHFs, determines a higher intensity of erosion and transport processes compared to deposition than in the other sites. Hummocks are generally larger in flat areas such as valley floors, whereas in steeper slopes and submittal locations the size of hummock is usually smaller (Pemberton, 1980; Ogata, 2005; 2007). Therefore, a less favorable topographic position could explain the smaller size of hummocks in the EHF-1, which however is the oldest field (Figure 7; Table 1).

It should be noted that the age of formation of the three EHFs does not correspond to the deglaciation age of the Zackenberg Valley that took place around ca. 8 ka (Vinther et al., 2009; Cable et al., 2018). Nevertheless, the age of the landforms seem to influence the size of earth hummocks, as suggested by the comparison between the data from the EHF-2 and the EHF-3 (the youngest and the one with the shortest length and width of the landforms). Nevertheless, the EHF-2 includes the landforms with greater length and width, as well as maximum height, as a result of coalescing hummocks. Some of these cryogenic mounds present small collapses, with cracks in their edges resulting from internal pressures (Tarnocai and Zoltai, 1978; Grab, 2005a). The larger size of the features in the EHF-2 is related to the balance between the different factors that can influence in this sense: topography, age of formation, ground thermal conditions, snow regime and moisture availability. At the same time, the EHF-1, the oldest, contains the smallest features, so data suggests that the topographic context and geomorphologic constraints have a greater influence on the morphology and morphometrics of the earth hummocks. Therefore, their morphometric properties are consequence of a multifactorial process as also suggested in other specific studies (e.g. Kojima, 1994; Van Vliet-Lanoë and Seppälä, 2002; Grab, 2005a, 2005b). In sum, hummocks can be considered polygenetic features that can be found in very different environments (Killingbeck and Ballantyne, 2012).

The mean maximum height (22 cm) is slightly below the averages observed in other studies conducted at high latitude regions, such as the Subarctic Canada and Finnish Lapland, where heights exceed 40 cm (Tarnocai and Zoltai, 1978; Luoto and Sepälä, 2002). In the Zackenberg Valley, the heights of earth hummocks are similar to those described in mountainous areas of mid-latitude regions, such as South West England, Northern Japan, or the Rocky Mountains (Scotter and Zoltai, 1982; Ogata, 2005; 2007; Killingbeck and Ballantyne, 2012).

However, although the largest hummocks are generally located in the high latitude areas (Grab, 2005), there are exceptions such as in Iceland, where morphometric parameters of earth hummocks (height, width and length) are very similar to our study case (Gerrard, 1992). In some of these subarctic and mid-latitude studied areas there is no permafrost. Several studies show that earth hummocks also develop in permafrost-free environments (Van Vliet-Lanoë et al., 1998; Killingbeck and Ballantyne, 2012). Thus, this reinforces the idea that different factors, many of them local in nature such as slope and altitude, can influence the development and morphometric characteristics of earth hummocks.

Similarly to other studies in which the L/W ratio was 1.23 (Ogata, 2007) or 1.5 (Killingbeck and Ballantyne, 2012), earth hummocks in NE Greenland define roughly elliptical forms (1.31 L/W ratio). In those elliptical/irregular hummocks, generally coalescent features, the longitudinal axis show a perpendicular direction with respect to the drainage flow. The perpendicular direction of the major axis of the hummocks is also related with the inclination, as hummocks usually tend to align their longest axes perpendicularly to the direction on the maximum slope (Pemberton, 1980).

Another important factor in the formation and development of earth hummocks is the presence of vegetation (Kojima, 1994; Pintaldi et al., 2016). In turn, the extent of type of vegetation cover is also a consequence of environmental and climatic conditions (Pintaldi et al., 2016). In fact, vegetation development is good in areas where earth hummocks develop well (Kojima, 1994). At the same time, the existence of a relationship between permafrost occurrence and vegetation height in earth hummocks has been demonstrated. Is the height of vegetation increases, permafrost occurrence decreases (Luoto and Seppälä, 2002). Therefore, the formation of these periglacial landforms must be understood as a complex cycle with many local and regional forcings favouring or reducing their growth. In the Zackenberg Valley, no significant changes on vegetation cover have been detected among the three EHFs, except for the slightly greater presence of mosses in the upper part of several hummocks in the EHF-2. Remarkably, microtopography exerts a strong control on the type of vegetation as hummocks are dominated by grasses and *Salix arctica*, whereas in the poorly drained interhummocks mosses abound.

**5.3. Spatial variability in soil properties and soil classification**

As a result of the geomorphological setting and topographical conditions, the type and intensity of soil processes prevailing in the EHFs show significant differences, which also affect the development of the earth hummocks. The three soils belong to the Cryosol group; due to the presence of a cryic horizon, a perennially frozen horizon less than one meter below the surface (IUSS Working Group WRB, 2006). Sections EH-1 and EH-2 can be classified as Glacic Reductaquic Cryosols (Loamic), mainly due to their sandy texture, while section EH-3 corresponds to a Glacic Reductaquic Cryosol (Silty). This difference in soil nomenclature at the level of the second qualifier according to the IUSS Working Group WRB (2016) contributes to the distinction between two different geochemical and sedimentary environments.

The greater amounts of silt and clay present in EH-3 seem to suggest that this area corresponds to a depositional environment for fine sediments (silt and clay), washed from the slope and moraine deposits and the upper hummock fields (EH-1 and EH-2) by a very low energy erosion system. Snow melting waters have an important role as a particle transport agent. The existence of a highly variable snow cover is considered a key factor in the development of these features as it controls water supply, the duration and depth of the active layer, the vegetation cycle, etc. (Kojima, 1994; Van Vliet-Lanoë and Seppälä, 2002).

A clear Mn enrichment was also observed in the subsurface horizons of section EH-3, which is consistent with the environmental implications of redox processes in soil. Mn oxides are characterized by a great specific surface area and a low degree of crystallinity (Burdige, 1993); therefore, under reducing conditions, Mn (IV) oxides are easily reduced to $Mn^{2+}$ (see e.g. Sposito et al., 1989). $Mn^{2+}$ stays in solution and can move with the water out of the soil (Vepraska and Faulkner, 2001), due to its slow oxidation kinetics, especially at pH < 8.5 (Stumm and Morgan, 1981; Thamdrup et al., 1994). Hence, loss of Mn may be particularly important in EH-1 and EH-2 soils because drainage is persisting in more elevated zones, where these two soils are located. The much lower concentrations of total Mn and MnOx (Table 3; Supplementary material) in EH-1 and EH-2 soils than in those located in the lower portion (EH-3) of the transect tend to support this hypothesis.

Thus, the sedimentary environment influences geochemical characteristics of the three EHFs. In turn, the sedimentary environment is conditioned by the topographic and geomorphological characteristics of each site. In the case of EHF-1 and 2, their location in the intermediate sector of the eastern slopes of the Zackenberg Valley connecting with Aucella Peak, determines the unique origin of the sedimentary contributions of these slopes. On the other hand, the EHF-3, located at the bottom of the Zackenberg Valley, receives both lateral sedimentary contributions from the above-mentioned slopes, and longitudinal contributions from the main valley.

The high concentrations of Mn found in EH-3 appear to suggest that part of the dissolved Mn in drainage waters could be retained either by oxidation and subsequent precipitation as an oxide or by adsorption onto Fe oxyhydroxides (Otero et al., 2009). Fe oxyhydroxides are also reduced, as indicated by the grey or greenish mottles present in the three sections (Montgomery et al., 2001). However, unlike Mn, Fe only experiences segregation within the section itself, while it quickly precipitates upon contact with oxygen as an amorphous Fe(III) oxyhydroxide (Vepraskas, 2001; Montgomery et al., 2001). The high concentrations of amorphous Fe oxyhydroxides observed in the three sections support this idea.

On the other hand, higher concentrations of silt and Mn give the soil in hummock field EH-3 a greater chemical reactivity, which explains its higher retention capacity for macro- and micronutrients such as P and Co and, presumably, N, as suggested by the high total N content. The higher nutrient concentrations are consistent with higher plant productivity levels, which could explain the higher organic matter content in hummock field EH-3 than EH-1 and EH-2 where the P concentration was very low.

Therefore, the obtained results show that, despite the proximity of the three hummock fields, there is spatial variability in terms of soil composition and properties, with clear implications for the system's primary productivity and capacity for C storage and stabilization.

Previous works have established that the melting of ice sheets in Antarctic (Raiswell et al., 2006, 2008a, b) and Arctic glaciers (Raiswell and Canfield, 2012), as well as of ice residing deep below the surface, can further contribute to the biogeochemical enrichment of coastal ecosystems (Nowak et al., 2018). In this sense, our results suggest that the thawing process associated with a global temperature increase can lead to the reactivation of mineralization of organic matter and redox processes, ultimately promoting the mobilization of biolimiting elements from land to coastal waters (Otero et al., 2009, Nowak et al., 2018). The potential export of these elements (Co, P, Fe...), either dissolved or forming colloids, and organic carbon (Cw) to coastal waters can have implications for coastal productivity (Statham et al., 2008, Otero et al., 2009, 2013).

## 6. Conclusions

Earth hummocks in the Zackenberg Valley are widespread in relatively flat areas, particularly between MS left by Late Quaternary glaciers. Their formation is, however, much younger than the moraines, and they formed during the Late Holocene (dates of basal organic layers between 615 ± 25 and 1755 ± 60 cal yr BP). These periglacial features include an alternation between organic and mineral layers, suggesting significant geomorphological changes in the local environmental setting during the last millennia.

The formation of these polygenetic landforms results from a complex balance between climate and microtopographical conditions, which leads to substantial differences in their morphological development. Moreover, this variability significantly affects the degree of edaphic development and composition of earth hummocks. Although the geological substrate was similar, composition and reactivity of its components showed two different geochemical environments. Fields EHF-1 and EHF-2 were similar, while field EHF-3, located at the bottom of the slope, was characterized by a higher degree of edaphic development, which translates into a higher concentration of reactive organic matter (i.e.

water-soluble C), of biolimiting elements (N, P; and Co), and of Mn oxides and hydroxides.

Considering that hummocks in EHF-3 are the youngest in this sequence, the results suggest that hummock fields can evolve towards a system with a higher geochemical reactivity in a relatively short period of time. This process can be promoted by microtopographical conditions (e.g. position of soils in the landscape) and by global warming. This evolution will have clear environmental implications, such as increased mobility and bioavailability of nutrients and organic C, both in terrestrial and aquatic environments (e.g. rivers and coastal waters).

**Acknowledgements**

The authors are grateful to Zackenberg Polar Research Station for providing logistic support for the field work. Marc Oliva is supported by the Ramón y Cajal Program (RYC-2015-17597) and the Research Group ANTALP (Antarctic, Arctic, Alpine Environments; 2017-SGR-1102) funded by the Government of Catalonia through the AGAUR agency. The work was funded by the PALEOGREEN (CTM2017-87976-P) project of the Ministry of Economy of Spain. The Consellería de Educación, Universidade e Formación Profesional-Xunta de Galicia (Axudas á consolidación e estruturación de unidades de investigación competitivas do SUG del Plan Galego IDT, Ambiosol Group, ref. 2018-PG036).

## References


Aoyama, M. (2005). Rock glaciers in the northern Japanese Alps: palaeoenvironmental implications since the Late Glacial. *Journal of Quaternary Science*, 20 (5), 471-484.

Bascomb, C.L. (1968). Distribution of pyrophosphate-extractable iron and organic carbon in soils of various groups, *Journal of Soil Science*, 19, 251–268, doi:10.1111/j.1365-2389.1968.tb01538.x.

Bay, C. (1998). *Vegetation mapping of Zackenberg valley, Northeast Greenland*. Danish Polar Center and Botanical Museum, University of Copenhagen (Denmark), 75 pp.

Bennike, O., Wagner, B. (2012). Deglaciation chronology, sea-level changes and environmental changes from Holocene lake sediments of Germania Havn Sø, Sabine Ø, northeast Greenland. *Quaternary Research*, 78, 103–109. DOI: 10.1016/j.yqres.2012.03.004

Blakemore, L.C. (1983). Acid oxalate-extractable iron, aluminium and silicon, ICOMAND. *Circular Letters,* 5, 1983.

Brown, J., Ferrians, O.J.J., Heginbottom, J.A., Melnikov, E.S. (1997). *Circum-Arctic Map of Permafrost and Ground-Ice Conditions*. US Geological Survey Reston.

Burdige, D.J. (1993). The biogeochemistry of manganese and iron reduction in marine sediments. *Earth-Science Reviews,* 35, 249–284.

Burn, C.R. (1990). Implications for palaeoenvironmental reconstruction of recent ice-wedge development at Mayo, Yukon Territory. *Permafrost and Periglacial Processes*, 1 (1), 3-14.

Cable, S., Christiansen, H.H., Westergaard-Nielsen, A., Kroon, A, Elberling, B. (2018). Geomorphological and cryostratigraphical analyses of the Zackenberg Valley, NE

Greenland and significance of Holocene alluvial fans. *Geomorphology*, 303, 504–523. DOI: 10.1016/j.geomorph.2017.11.003

Cannone, N., Wagner, D., Hubberten, H.W.W., Guglielmin, M. (2008). Biotic and abiotic factors influencing soil properties across a latitudinal gradient in Victoria Land, Antarctica. *Geoderma*, 144, 50–65, doi:10.1016/j.geoderma.2007.10.008.

Christiansen, H.H., Sigsgaard, C., Humlum, O., Rasch, M., Hansen, B.U. (2008). Permafrost and periglacial geomorphology at Zackenberg. *Advances in Ecological Research*, 40, 151–174. DOI: 10.1016/S0065-2504(07)00007-4.

Costin, A.B., Wimbush D.J. (1973). Frost Cracks and Earth Hummocks at Kosciusko, Snowy Mountains, Australia. *Arctic and Alpine Research*, 5:2, 111–120. DOI: 10.1080/00040851.1973.12003685

Elberling, B., Michelsen, A., Schädel, C., Schuur, E.A., Christiansen, H.H., Berg, l., Tamstorf, M.P., Sigsgaard, C. (2013). Long-term CO2 production following permafrost thaw. *Nature Climate Change*, 3, 890–894.

Elliott, G., Worsley, P. (1999). The sedimentology, stratigraphy and 14C dating of a turf-banked solifluction lobe: evidence for Holocene slope instability at Okstindan, northern Norway. *Journal of Quaternary Science*, 14 (2), 175-188.

Ellis, E. (1983). Stratigraphy and 14C Dating of Two Earth Hummocks, Jotunheimen, South Central Norway. *Geografiska Annaler. Series A, Physical Geography*, 65 (3/4), 279–287.

French H. (2007). *The Periglacial Environment*. 3rd edition. Wiley, Chichester, UK.

Gee, G.W., Bauder, J.W. (1986). Particle-size analysis, In: *Methods of soil analysis, edited by K.A.*, American Society of Agronomy and Soil Science Society of America, Madison, 383–412.

Gerrard, J. (1992). The nature and geomorphological relationships of earth hummocks (thufa) in Iceland. *Zeitschrift für Geomorphologie*, 86, 173–182.

Gillespie A.W., Sanei H., Diochon A., Ellert B.H., Regier T.Z., Chevrier D., Dynes J.J., Tarnocai C., Gregorich E.G. (2014). Perennially and annually frozen soil carbon differ in their susceptibility to decomposition: Analysis of Subarctic earth hummocks by bioassay, XANES and pyrolysis. *Soil Biology & Biochemistry*, 68, 106–116. DOI: 10.1016/j.soilbio.2013.09.021

Grab, S. (2005a). Earth hummocks (thúfur): new insights to their thermal characteristics and development in eastern Lesotho, southern Africa. *Earth Surface Processes and Landforms,* 30, 541–555. DOI: 10.1002/esp.1150

Grab, S. (2005b). Aspects of the geomorphology, genesis and environmental significance of earth hummocks (thúfur, pounus): miniature cryogenic mounds. *Progress in Physical Geography: Earth and Environment*, 29 (2), 139–155. DOI: 10.1191/0309133305pp440ra

Gurney, S.D., Hayward, S. (2014). Earth hummocks in north-east Okstindan, northern Norway: Morphology, distribution and environmental constraints. *Norsk Geografisk Tidsskrift - Norwegian Journal of Geography*, 69, 299–309. DOI: 10.1080/00291951.2015.1084530

Hall, G.E.M., Vaine, J.E., MacLaurin, A.I. (1996). Analytical aspects of the application of sodium pyrophosphate reagent in the specific extraction of the labile organic component of humus and soils. *Journal of Geochemical Exploration*, 56, 23–36.

Hansen, B.U., Sigsgaard, C., Rasmussen, L., Cappelen, J., Hinkler, J., Mernild, S.H., Petersen, D., Tamstorf, M.P., Rasch, M., Hasholt, B. (2008). Present-day climate at Zackenberg. *Advances in Ecological Research*, 40, 111–149. DOI: 10.1016/S0065-2504(07)00006-2.

Higgins, A.K. (2003). *East Greenland 70º – 82º N. Geological Map 1:1,000,000.* The Geological Survey of Denmark and Greenland, Copenhagen.

Højlund Pedersen, S. (2017). *Scaling-up Climate Change Effects in Greenland*. PhD Thesis 2017. Aarhus University, Denmark.

IUSS Working Group WRB. (2006). *World reference base for soil resources 2006*. 2nd edition. World Soil Resources Reports No. 103. FAO, Rome.

Killingbeck, J., Ballantyne, C.K. (2012). Earth Hummocks in West Dartmoor, SW England: Characteristics, Age and Origin. *Permafrost and Periglacial Processes*, 23, 152–161.

Kojima, S. (1994). Relationships of vegetation, earth hummocks, and topography in the High Artic environment of Canada. Proc. NIPR Symp. *Polar Biology*, 7, 256–269.

Kokelj, S.V., Burn C.R., Tarnocai C. (2007). The Structure and Dynamics of Earth Hummocks in the Subarctic Forest Near Inuvik, Northwest Territories, Canada, *Arctic, Antarctic, and Alpine Research*, 39 (1), 99–109. DOI: 10.1657/1523-0430(2007)39[99:TSADOE]2.0.CO;2

Kottek, M., Grieser, J., Beck, C., Rudolf, B., Rubel, F. (2006). Word map of the Köppen-Geiger climate classification updated. *Meteorologische Zeitschrift*, 15 (3), 259–263.

Luoto, M., Seppälä, M. (2002). Characteristics of earth hummocks (pounus) with and without permafrost in Finnish Lapland. *Geografiska Annaler. Series A Physical Geography*, 84 (2), 127–136. DOI: 10.1111/1468-0459.00166

Luoto, M., Seppälä, M. (2003). New extensive sporadic permafrost feature in Finnish Lapland: peaty earth hummocks (pounus). In: *Permafrost, Phillips, Springman, Arenson (Eds)*, Swets & Zeitlinger, Lisse, 703–705.

Mackay, J.R. (1980). The origin of hummocks, western Arctic coast, Canada. *Canadian Journal of Earth Sciences*, 17 (8), 996–1006. DOI: 10.1139/e80-100

Mackay, J.R., MacKay, D.K. (1976). Cryostatic pressures in nonsorted circles (mud hummocks), Inuvik, Northwest Territories. *Canadian Journal of Earth Sciences*, 13 (7), 889–897. DOI: 10.1139/e76-092

McKay, N.P., Kaufman, D.S., Routson, C.C., Erb, M.P., Zander, P.D. (2018). The Onset and Rate of Holocene Neoglacial Cooling in the Arctic. *Geophysical Research Letters*, 45, 12,487–12,496. DOI: 10.1029/2018GL079773

Mehlich, A. (1984). Mehlich 3 soil test extractant: a modification of the Mehlich 2 extractant. Commun. *Communications in Soil Science and Plant Analysis*, 15, 1409–1416.

Mehra, O.P., Jackson, M.L. (1960). Iron oxide removal from soils and clays by a dithionite-citrate system buffered with sodium bicarbonate. In: *Proceedings 7th National Conference on Clays*, 5, 317–327.

Milošević, M.V., Milivojević, M., Ćalić, J. (2007). Earth hummocks in the regions of Vlasina and Krajište (Southern Serbia). *Bulletin of the Serbian Geographical Society*, T. LXXXVII (1), 39–50.

Montgomery, J.A., Tandarich, J.P., Whited, P.M. (2001). *Use of soil information for hydrogeomorphic assessment.* In Richardson, J.L., Vepraskas, M.J. (Eds.), Wetland soils. Genesis, hydrology, landscapes and classification,CRC press. Boca Raton, pp. 229-267.

Murphy, J., Riley, J.P. (1962). A modified single solution method for the determination of phosphate in natural waters. *Analytica Chimica Acta*, 27, 31–36.

Nowak A, Hodson A., Turchyn A.V. (2018) Spatial and Temporal Dynamics of Dissolved Organic Carbon, Chlorophyll, Nutrients, and Trace Metals in Maritime

Antarctic Snow and Snowmelt. Front. Earth Sci. 6:201. doi: 10.3389/feart.2018.00

Ogata, T. (2005). Peaty hummocks as an environmental indicator: a case of Japanese upland mire. *Tsukuba Geoenvironmental Sciences*, 1, 33–38.

Ogata, T. (2007). Morphology and Environmental Factors of Periglacial Hummocks in the Nemuro Peninsula, Northern Japan. *Geographical Review of Japan*, 80 (5), 246–258.

Oliva, M., Gómez-Ortiz, A. (2012). Late Holocene environmental dynamics and climate variability in a Mediterranean high mountain environment (Sierra Nevada, Spain) inferred from lake sediments and historical sources. *The Holocene*, 22 (8): 915-927.

Oliva, M., Schulte, L., Gómez-Ortiz, A. (2011). The role of aridification in constraining the elevation range of Holocene solifluction processes and associated landforms in the periglacial belt of the Sierra Nevada (southern Spain). *Earth Surface Processes and Landforms*, 36, 1279–1291. DOI: 10.1002/esp.2116

Oliva, M., Vieira, G., Pina, P., Pereira, P., Neves, M., Freitas, M.C. (2014). Sedimentological characteristics of ice-wedge polygon terrain in Adventdalen (Svalbard)–environmental and climatic implications for the late Holocene. *Solid Earth*, 5 (2), 901–914.

Otero, X.L., Fernández, S., de Pablo Hernandez, M.A., Nizoli, E.C., Quesada, A. (2013). Plant communities as a key factor in biogeochemical processes involving micronutrients (Fe, Mn, Co, and Cu) in Antarctic soils (Byers Peninsula, maritime Antarctica). *Geoderma*, 195–196, 145–154. DOI: 10.1016/j.geoderma.2012.11.018.

Otero, X.L., Ferreira, T.O., Huerta-Díaz, M.A., Partiti, C.S.M., Souza Jr., V., Vidal, P., Macías, F. (2009). Geochemistry of iron and manganese in soils and sediments of a mangrove system, Island of Pai Matos (Cananeia, SP, Brazil). *Geoderma*, 148, 310–335.

Otero, X.L., Tierra, W., Atiaga, O., Guanoluisa, D., Nunes, L.M., Ferreira, T.O., Ruales, J., (2016). Arsenic in rice agrosystems (water, soil and rice plants) in Guayas and Los Ríos provinces, Ecuador. *Science of The Total Environment*. 573, 778–787. DOI: 10.1016/j.scitotenv.2016.08.162

Pedersen, M., Weng, W.L., Keulen, N.T., Kokfelt, T. (2013). A new seamless digital 1:500.000 geological map of Greenland. *Geological Survey of Denmark and Greenland Bulletin,* 28, 65–68.

Pemberton, M. (1980). Earth hummocks at low elevation in the Vale of Eden, Cumbria. *Transactions of the Institute of British Geographers*, 5 (4), 487–501.

Pintaldi, E., D'Amico, M.E., Siniscalco, C., Cremonese, E., Celi, L., Filippa, G., Prati, M., Freppaz, M. (2016). Hummocks affect soil properties and soil-vegetation relationships in a subalpine grassland (North-Western Italian Alps). *Catena,* 145, 214–226. DOI: 10.1016/j.catena.2016.06.014

Quinton, W.L., Marsh P. (1998). The Influence of Mineral Earth Hummocks on Subsurface Drainage in the Continuous Permafrost Zone. *Permafrost and Periglacial Processes*, 9, 213–228.

Raiswell, R., Tranter, M., Benning, L.G., Siegert, M., De'ath, R., Huybrenchts, P., Payne, T., (2006). Contributions from glacially derived sediments to the global iron (oxyhydr)oxide cycle: implications for iron delivery to the oceans. Geochimica et CosmochimicaActa 70, 2765–2780.

Raiswell, R., Benning, L.G., Tranter, M., Tulaczyk, S. (2008a) Bioavailable iron in the Southern Ocean: The significance of the iceberg conveyor belt. Geochemical Transactions 9, 7.

Raiswell, R., Benning, L.G., Davidson, L, Tranter, M. (2008b) Nanoparticulate bioavailable iron minerals in icebergs and glaciers. Mineralogical Magazine 72, 345-348.

Raiswel, R., Canfield, D. (2012). The ion biogeochemical cycle past and present Geochemical Perspectives 1(1): 1-220. European Association of Geochemistry.

Reimer, P.J., Bard, E., Bayliss, A., Beck, J.W., Blackwell, P.G., Bronk-Ramsey, C., Buck, C.E., Cheng, H., Edwards, R.L., Friedrich, M., Grootes, P.M., Guilderson, T.P., Haflidason, H., Hajdas, I., Hatte, C., Heaton, T.J., Hoffmann, D.L., Hogg, A., Hughen, K.A., Kaiser, K.F., Kromer, B., Manning, S.W., Niu, M., Reimer, R.W., Richards, D.A., Scott, E.M., Southon, J.R., Staff, R.A., Turney, C.S.M., van der Plicht, J. (2013). IntCal13 and Marine13 radiocarbon age calibration curves 0e50,000 years cal BP. *Radiocarbon*, 55 (4), 1869-1887. DOI: 10.2458/azu_js_rc.55.16947.

Rowell, D. L. (1994). *Soil Science: Methods and applications.* Longman Scientific and technical, U.K.

Sarkar, A.N., Wynjones, R.G. (1982). Effect of rhizosphere pH on the availability and uptake of Fe, Mn and Zn. *Plant Soil*, 66 (3), 361–372, DOI:10.1007/BF02183802.

Scott, M.B., Dickinson, K.J.M., Barratt, B.I.P., Sinclair, B.J. (2008). Temperature and Moisture Trends in Non-sorted Earth Hummocks and Stripes on the Old Man Range, New Zealand: Implications for Mechanisms of Maintenance. *Permafrost and Periglacial Processes*, 19, 305–314. DOI: 10.1002/ppp.627

Scotter, G.W., Zoltai, S.C. (1982). Earth hummocks in the Sunshine area of the Rocky Mountains, Alberta and British Columbia. *Arctic*, 411–416.

Seppälä, M. (2005). Frost heave on earth hummocks (pounus) in Finnish Lapland. *Norsk Geografisk Tidsskrift - Norwegian Journal of Geography*, 59 (2) 171-176.

Sharp, R.P. (1942). Soils structures in the St. Elias Range, Yukon Territory. Journal of *Geomorphology*, 5, 274–301.

Sigsgaard, C., Thorøe, K., Lund, M., Kandrup, N., Larsen, M., Falk, J.M., Hansen, B.U., Ström, L., Christiensen, T.R., Tamstorf, M. (2009). Zackenberg Basic: The ClimateBasis and GeoBasis programmes. *Zackenberg Ecological Research Operations*. *15th Annual Report 2009*. National Environmental Research Institute, Aarhus University, Roskilde (Denmark), 12–35.

Sinclair, G., Carlson, A.E., Mix, A.C., Lecavalier, B.S., Milne, G., Mathias, A., Buizert, C., DeConto, R. (2016). Diachronous retreat of the Greenland ice sheet during the last deglaciation. *Quaternary Science Reviews*, 145, 243–258. DOI: 10.1016/j.quascirev.2016.05.040

Sposito, G. (1989). *The Chemistry of Soils*, Oxford University Press, New York.

Statham, P.J., Skidmore, M., Tranter, M. (2008). Inputs of glacially derived dissolved and colloidal iron to the coastal ocean and implications for primary productivity, Global Biogeochem. *Cycles*, 22, 11. DOI:10.1029/2007GB003106.

Stuiver, M., Reimer, P.J. (1993). Extended 14C Data Base and Revised CALIB 3.0 14C Age Calibration Program. *Radiocarbon*, 35(1), 215–230.

Stumm, W., Morgan, J.J. (1981). *Aquatic Chemistry.* John Wiley and Sons, New York.

Thamdrup, B., Fossing, H., Jørgensen, B.B. (1994). Manganese, iron, and sulfur cycle in a coastal marine sediment, Aahus Bay, Denmark. *Geochimica et Cosmochimica Acta,* 23, 5115–5129.

Sullivan, J.H., Woodall, W.H. (1996). A Control Chart for Preliminary Analysis of Individual Observations. *Journal of Quality Technology*, 28, 3, 265–278.

Tarnocai C., Zoltai S. C. (1978). Earth Hummocks of the Canadian Arctic and Subarctic. *Arctic and Alpine Research*, 10 (3), 581–594. DOI: 10.1080/00040851.1978.12003997

Van Vliet-Lanoë, B., Seppälä, M. (2002). Stratigraphy, age and formation of peaty earth hummocks (pounus), Finnish Lapland. *The Holocene*, 12 (2), 187–199. DOI: 10.1191/0959683602hl534rp

Van Vliet-Lanoë B, Bourgeois O, Dauteuil O. (1998). Thufur formation in northern Iceland and its relation to Holocene climate change. *Permafrost and Periglacial Processes*, 9, 347–365.

Vasskog, K., Langebroek, P.M., Andrews, J.T., Nilsen, J.E.Ø., Nesje, A. (2015). The Greenland Ice Sheet during the last glacial cycle: Current ice loss and contribution to sea-level rise from a palaeoclimatic perspective. *Earth-Science Rev*iews, 150, 45–67. DOI: 10.1016/j.earscirev.2015.07.006

Vepraskas, M.L. (2001). *Morphological features of seasonally reduced soil.* In Richardson, J.L., Vepraskas, M.J. (Eds), Wetland soils. Genesis, Hydrology, landscapes and classifiction,CRC press. Boca Raton, pp. 163-208.

Vepraska, M.J., Falkner, S.P. (2001). *Redox chemistry of hydric soils*. In Richarson, J.L., Vepraska, M.J. (eds.), Wetlands soils. Genesis, hydrology, landscape and classification. Boca Raton, CR Press, pp. 86–106.

Verret, M., Wang, Y., Bjornson, J., Lacelle, D. (2019). Hummocks in alpine tundra, northern British Columbia, Canada: distribution, morphology and organic carbon composition. *Arctic Science*, 5 (3), 127–147. DOI: 10.1139/as-2018-0021

Vinther, B.M., Buchardt, S.L., Clausen, H.B., Dahl-Jensen, D., Johnsen, S.J., Fisher, D.A., Koerner, R.M., Raynaud, D., Lipenkov, V., Andersen, K.K., Blunier, T., Rasmussen, S.O., Steffensen, J.P., Svensson, A.M. (2009). Holocene thinning of the Greenland ice sheet. *Nature*, 461, 385–388. DOI: 10.1038/nature08355.

Violante, A., Cozzolino,V., Perelomov, L., Caporale, A.G., Pigna, M. (2010). Mobility and bioavailability of heavy metals and metalloids in soil environmemts, *Journal of Soil Science and Plant Nutrition*, 10, 268–292.

Wagner, B., Bennike, O., Cremer, H., Klug, M. (2010). Late Quaternary history of the Kap Mackenzie area, northeast Greenland. *Boreas*, 39, 492–504.

Westermann, S., Elberling, B., Højlund Pedersen, S., Stendel, M., Hansen, B., Liston, G. (2015). Future permafrost conditions along environmental gradients in Zackenberg, Greenland. *The Cryosphere*, 9 (2), 719–735.

Winkler, S., Lambiel, C. (2018). Age constraints of rock glaciers in the Southern Alps/New Zealand–Exploring their palaeoclimatic potential. The Holocene, 28 (5), 778-790.

Zoltai, S.C., Pettapiece W.W. (1974). Tree Distribution on Perennially Frozen Earth Hummocks. *Arctic and Alpine Research*, 6 (4), 403–411. DOI: 10.1080/00040851.1974.12003796

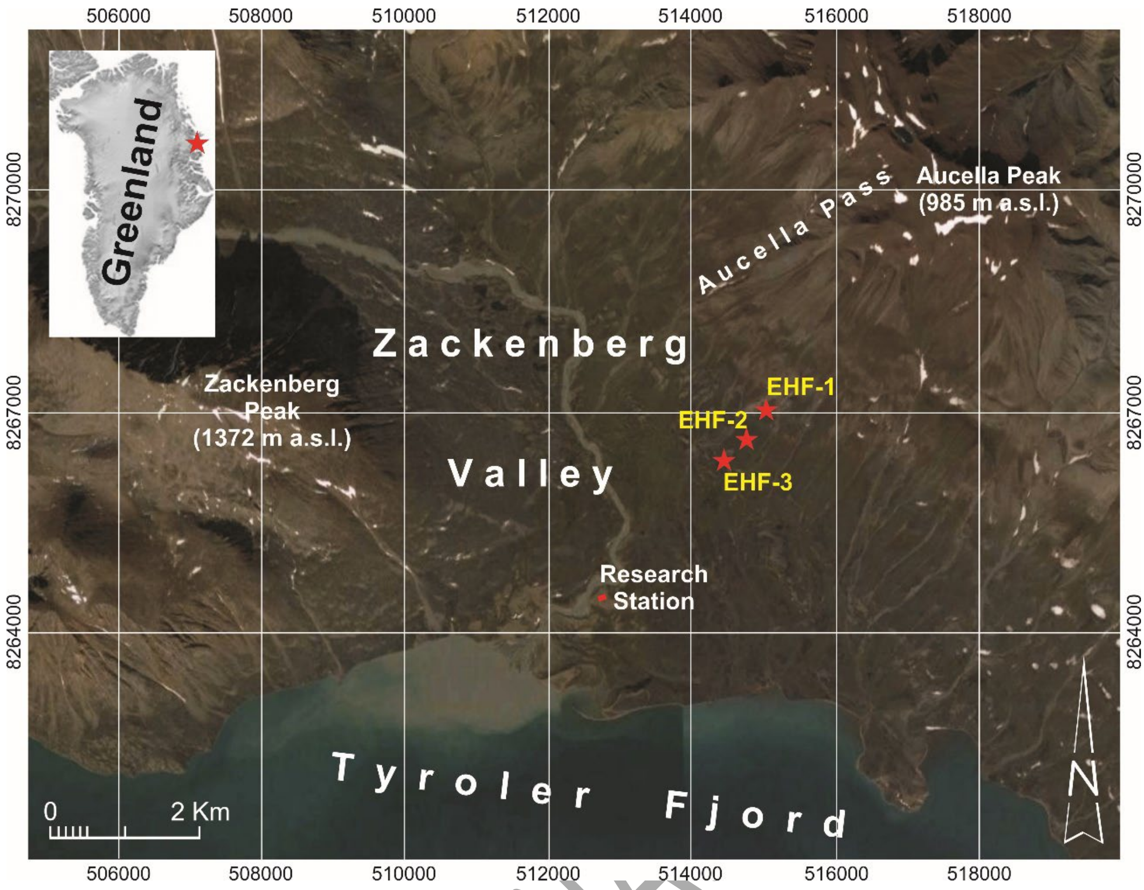


Figure 1. Location of the study area within the Zackenberg valley (NE Greenland; UTM Zone 27X). Source: Google Earth Imagery, 2012.

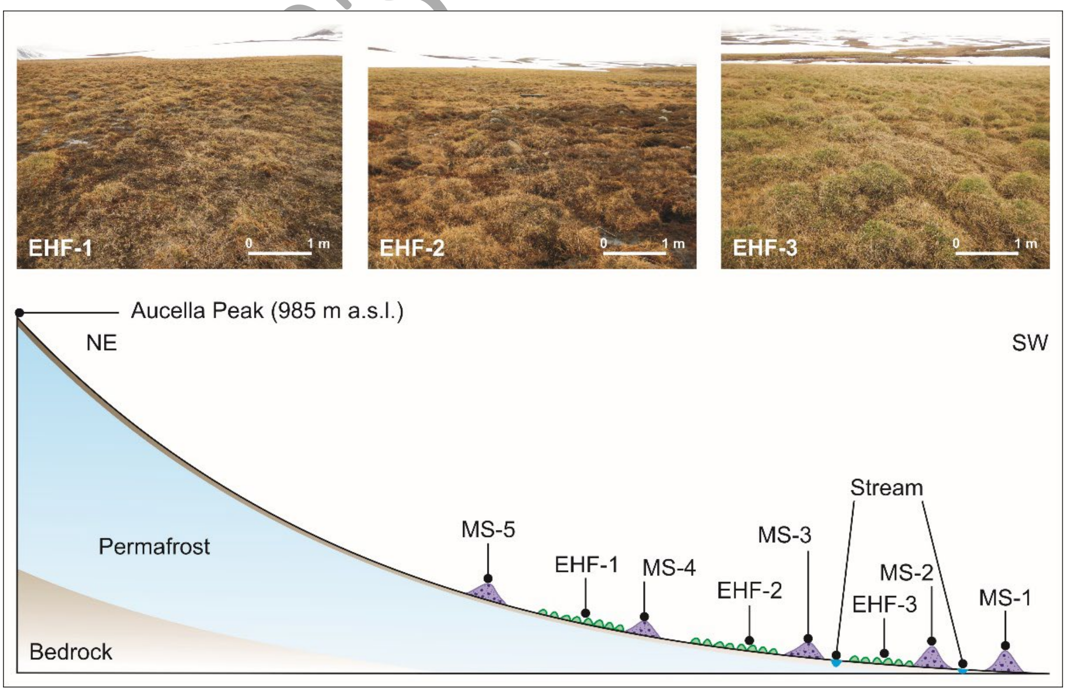


Figure 2. Geomorphological sketch showing the location of the three EHFs on the slope of the Aucella Peak (it is not to scale), together with pictures of each of them.

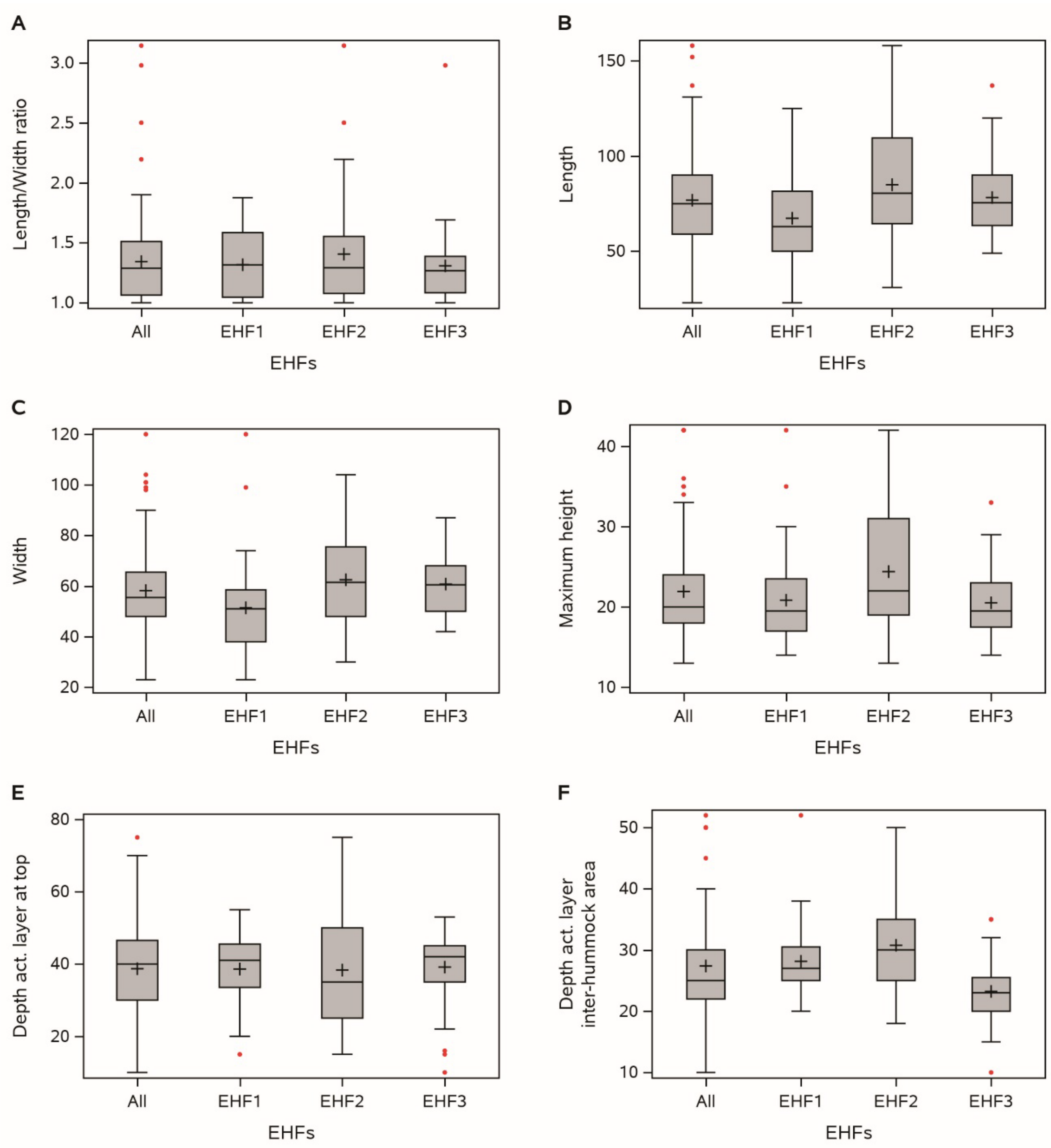


Figure 3. Distribution of (A) Length/Width ratio; (B) Length; (C) Width; (D) Maximum height; (E) Depth of the active layer at the top of the hummocks; (F) Depth of the active layer in the inter-hummock area. Total sample (All) and depending on the EHFs (EHF-1, EHF-2, EHF3). Units: cm. All statistical values, including upper and lower fence, have been included in Supplementary Table 1. Confidence intervals have been generated for the means of each variable (see Supplementary Table 1).

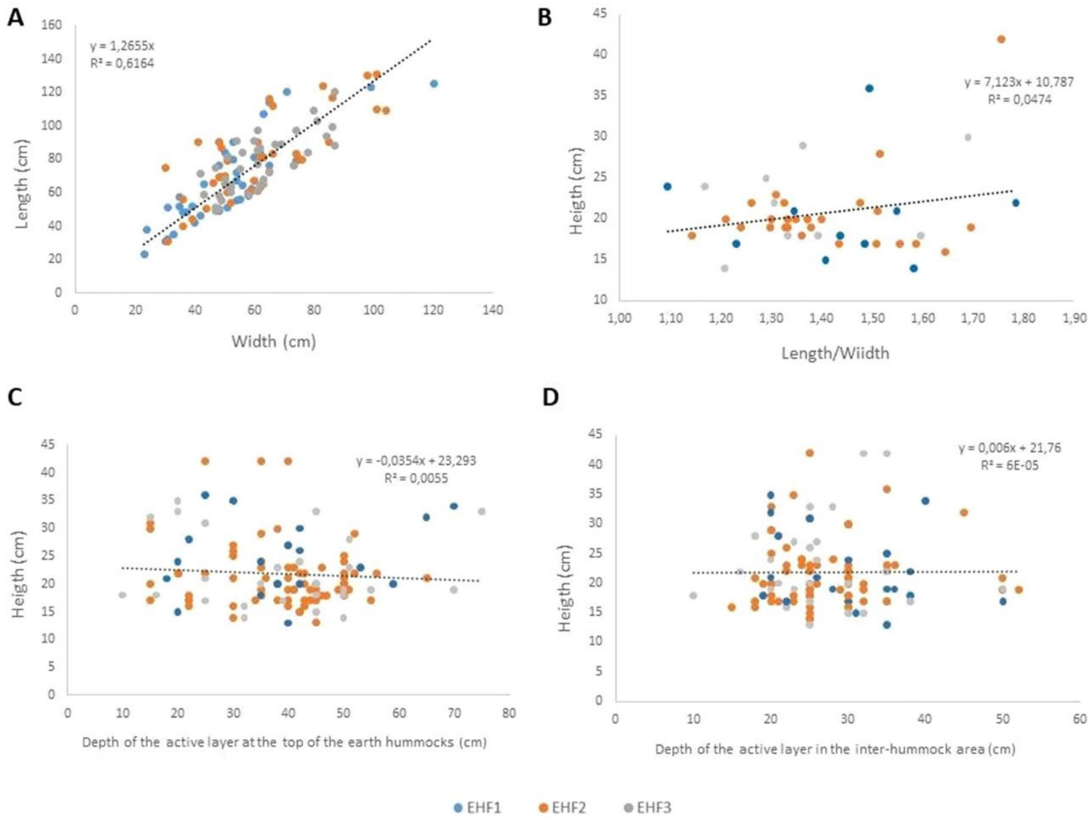


Figure 4. Linear regression showing the relationship between (A) L and W; (B) the ratio L/W and H1 in elliptical morphologies (C) AL-TOP and H1 (D) AL-BASE and H1.

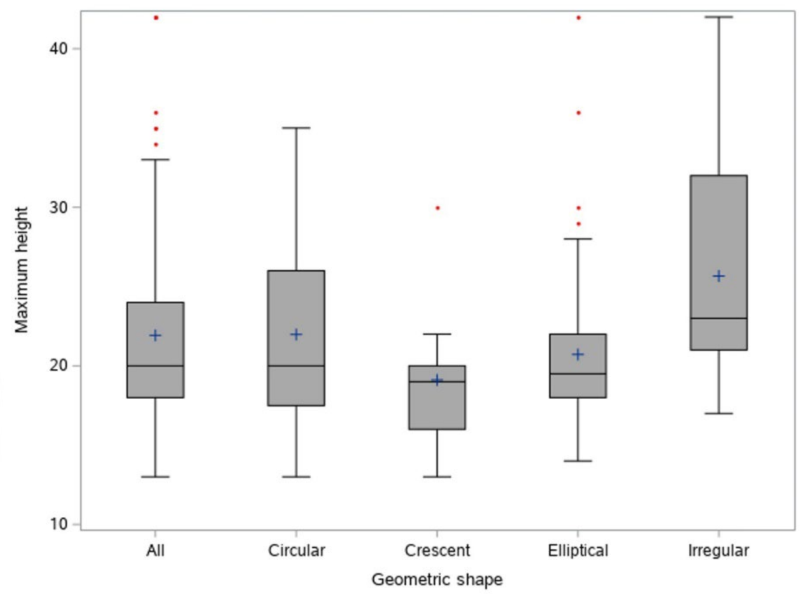


Figure 5. Distribution of Maximum height: total sample (All) and depending on the geometric shapes of the hummocks. Units: cm. All statistical values, including upper and lower fence, have been included in Supplementary Table 2. Confidence intervals have been generated for the means of each variable (see Supplementary Table 2).

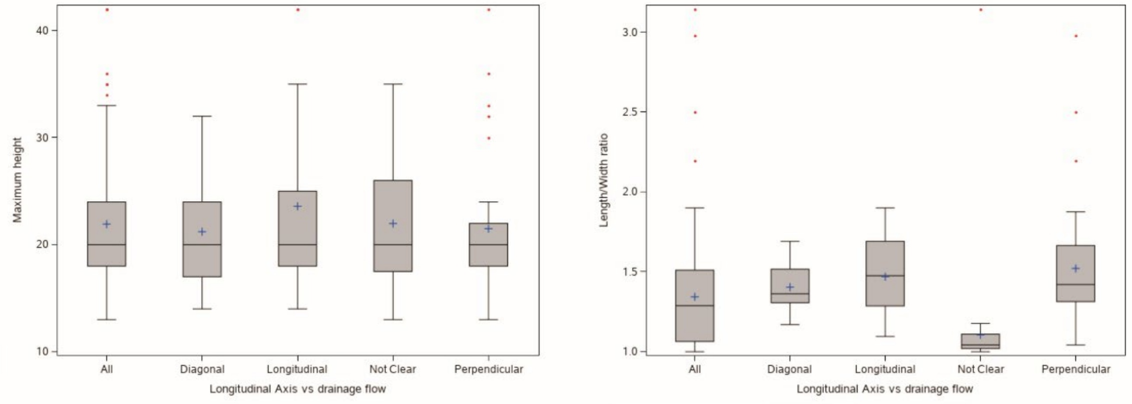


Figure 6. Distribution of (A) Maximum height; (B) Length/Width ratio. Depending on the direction of the longitudinal axis with respect to the drainage flow. Units: cm. All statistical values, including upper and lower fence, have been included in Supplementary Table 3. Confidence intervals have been generated for the means of each variable (see Supplementary Table 3).

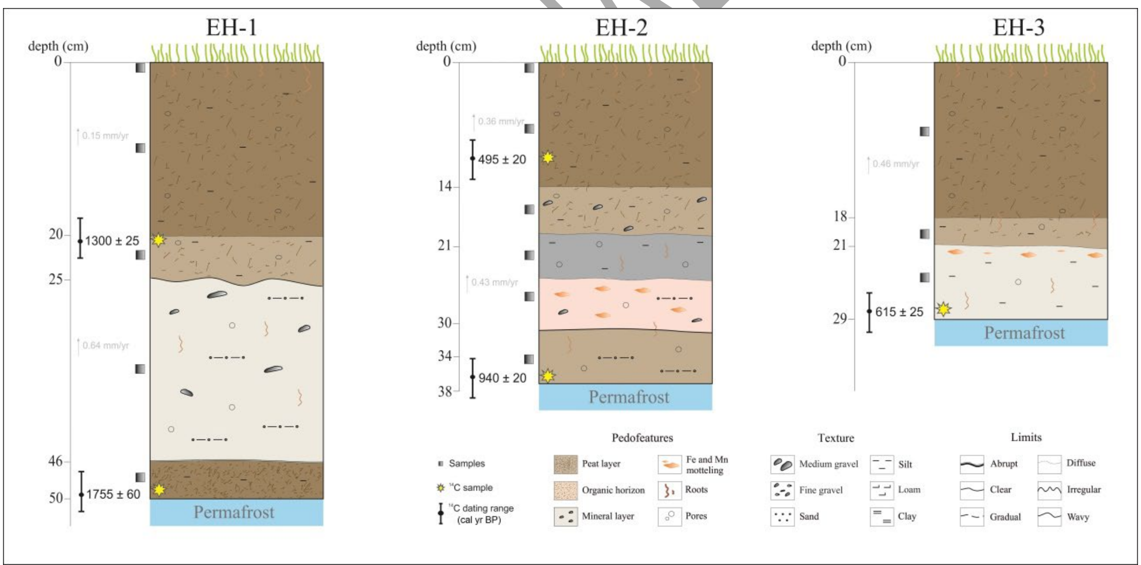


Figure 7. Lithostratigraphical sections of three earth hummocks.

Table 1. Radiocarbon dates of the three studied earth hummocks.

| Earth hummock | Lab Code | Depth (cm) | Material | $^{14}$C-years | $^{14}$C- years cal BP (1σ) | Calendar years BP (95,4 %) |
|---|---|---|---|---|---|---|
| EH-1 | ULA-8158 | 49 | bulk sediment | 1795 ± 20 | 1692-1814 | 1755 ± 60 |
| EH-1 | ULA-8159 | 20 | bulk sediment | 1375 ± 20 | 1275-1324 | 1300 ± 25 |
| EH-2 | ULA-8178 | 37 | bulk sediment | 1015 ± 15 | 920-960 | 940 ± 20 |
| EH-2 | ULA-8179 | 18 | bulk sediment | 425 ± 15 | 478-514 | 495 ± 20 |
| EH-3 | ULA-8160 | 28 | bulk sediment | 580 ± 20 | 589-641 | 615 ± 25 |
| EH-3 | ULA-8157 | 20 | bulk sediment | Modern | Modern | Modern |

Table 2. Mean values (±standard deviations,SD) and range for pH, total organic carbon (TOC), total nitrogen (TN), organic C soluble in sodium pyrophosphate (Cpyr), organic C soluble in water (Cw) and granulometry. Values in the same column indicated by different letters are significantly different, at p< 0.05.

| Site | pHw | EC | Sand | Silt | Clay | TOC | Cpyr | TN | Cw |
|---|---|---|---|---|---|---|---|---|---|
| | | µS cm$^{-1}$ | ------------------------------------------------%------------------------------------- | | | | | | mg kg$^{-1}$ |
| EH-1 | | | | | | | | | |
| mean±SD | 5.7±0.4$^{b}$ | 46±15$^{b}$ | 54±6$^{a}$ | 33±4$^{b}$ | 10±3$^{b}$ | 4.7±1.7$^{b}$ | 3.0±1.1$^{a}$ | 0.33±0.13$^{b}$ | 72±51$^{b}$ |
| range | 5.4-6.1 | 31-68 | 45-61 | 27-37 | 9-14 | 2.1-6.7 | 1.9-4.7 | 0.14-0.50 | 50-163 |
| EH-2 | | | | | | | | | |
| mean±SD | 5.7±0.7$^{b}$ | 55±26$^{b}$ | 54±11$^{a}$ | 39±8$^{b}$ | 7.3±3$^{b}$ | 5.0±3.8$^{b}$ | 3.4±2.3$^{a}$ | 0.33±0.24$^{b}$ | 110±50$^{b}$ |
| range | 5.1-6.9 | 31-104 | 42-71 | 27-47 | 2-12 | 0.31-1.6 | 0.4-7.5 | 0.01-0.70 | 50-348 |
| EH-3 | | | | | | | | | |
| mean±SD | 6.3±0.7$^{a}$ | 162±66$^{a}$ | 34±7$^{b}$ | 54±6$^{a}$ | 15±3$^{a}$ | 23±12$^{a}$ | 3.6±0.1$^{a}$ | 1.10±0.32$^{a}$ | 1072±358$^{a}$ |
| range | 5.5-7.0 | 87-212 | 26-41 | 48-59 | 10-17 | 10.3-34 | 3.5-3.7 | 0.76-1.35 | 818-1326 |

Table 3. Mean values (±standard deviations,SD) and range for total concentration of Fe, Al, Mn, P, Co and Cu and metal partitioning (FePy: iron associate to organic matter; FeOX: amorphous iron oxyhydroxides; FeD: crystalline iron oxyhydroxides). Values in the same column indicated by different letters are significantly different, at p< 0.05.

| Site | TFe | TAl | TMn | TP | TCo | TCu | FePy | FeOx | FeD | MnOx |
|---|---|---|---|---|---|---|---|---|---|---|
| | -----------%-------- | | ----------------------mg kg-1----------------------- | | | | ---------------------%--------------------- | | | mg kg-1 |
| EH-1 | | | | | | | | | | |
| mean±SD | 3.8±0.5[a] | 2.1±0.2[a] | 463±80[b] | 68±4[b] | 18±3[b] | 55±9[a] | 0.32±0.04[a] | 0.32±0.7[a] | 0.60±0.24[a] | 213±62[b] |
| range | 3.4-4.5 | 1.9-2.4 | 631-547 | 63-73 | 15-22 | 47-66 | 0.24-0.35 | 0.24-0.58 | 0.32-1.05 | 120-314 |
| EH-2 | | | | | | | | | | |
| mean±SD | 3.2±1.2[a] | 1.8±0.9[a] | 709±634[b] | 63±29[b] | 21±2.2[b] | 49±9[a] | 0.35±0.17[a] | 0.39±0.20[a] | 0.79±0.29[a] | 512±520[b] |
| range | 0.7-3.9 | 0.1-3.0 | 265-1960 | 8-96 | 19-24 | 36-61 | 0.02-0.54 | 0.26-0.64 | 0.20-1.01 | 134-1861 |
| EH-3 | | | | | | | | | | |
| mean±SD | 2.4±1[a] | 1.5±0.9[a] | 8226±8092[a] | 77±16[a] | 61±42[a] | 55±29[a] | 0.21±0.17[a] | 0.21±22[a] | 0.57±0.13[a] | 4883±3166[a] |
| range | 1.1-3.0 | 0.9-2.6 | 1440-19600 | 60-92 | 15-145 | 37-87 | 0.04-0.38 | 0.26-0.57 | 0.38-0.66 | 1721-9210 |

Table 4. Concentration of bioavailability fraction of macro (P) and micronutrients (Fe, Mn, Co and Cu) (soluble in Mehlich extraction, Me) and Co and Cu associated to organic matter (soluble in pyrophosphate, Py). Values in the same column indicated by different letters are significantly different, at p< 0.05.

| Site | PMe | FeMe | MnMe | CoMe | CuMe | CoPy | CuPy |
|---|---|---|---|---|---|---|---|
| | ------------------------------------------------mg kg-1------------------------------------------------ | | | | | | |
| EH-1 | | | | | | | |
| mean±SD | 1.1±1.4[b] | 354±38[a] | 28±14[b] | 0.7±0.2[b] | 7.1±3[b] | 2.3±0.8[a] | 14±5.8[a] |
| range | 0.33-3.6 | 338-444 | 12-47 | 0.6-1.0 | 4.8-13 | 1.0-3.0 | 8-22 |
| EH-2 | | | | | | | |
| mean±SD | 0.6±0.4[b] | 530±301[a] | 43±61[b] | 0.9±0.2[b] | 2.8±1.5[b] | 1.0±0[a] | 8.4±5[a] |
| range | 0.2-1.4 | 364-1140 | 11-169 | 0.7-1.2 | 0.5-4.4 | 1.0- <LD | 1-17 |
| EH-3 | | | | | | | |
| mean±SD | 14±5[a] | 914±871[a] | 533±472[a] | 3.2±2.8[a] | 10±14[a] | 19±11[a] | 19±9.5[a] |
| range | 11-18 | 200-1885 | 180-1070 | 1.7-6.5 | 2-27 | 1.0-24 | 2-18 |